

Solar corona during the 1994 and 1999 eclipses

O.G. Badalyan¹ and J. Sýkora²

¹ *Pushkov Institute of Terrestrial Magnetism, Ionosphere and Radio Wave Propagation, 142190 Troitsk, Moscow Region, Russia,
(E-mail: badalyan@izmiran.troitsk.ru)*

² *Astronomical Institute of the Slovak Academy of Sciences
059 60 Tatranská Lomnica, The Slovak Republic,
(E-mail: sykora@ta3.sk)*

Received: December 20, 2007; Accepted: January 22, 2008

Abstract. The lower and middle layers of the corona are studied analyzing the ground-based observations carried out during the November 3, 1994 and August 11, 1999 total solar eclipses. While the 1994 eclipse took place nearby the solar activity minimum, the 1999 eclipse occurred closer to the solar cycle maximum. Structures, isolines of brightness and polarization, and topology of the magnetic field lines of force (calculated under a potential approximation) of these two coronae are mutually compared. It is confirmed that the brightness distribution in the corona corresponds to the hydrostatic distribution of density at the distances $1.2 - 1.8 R_{\odot}$. Temperature 1.4 MK and density $n_0 = 3.3 \times 10^8 \text{ cm}^{-3}$ are found for the equatorial coronal regions of the 1999 corona. Physical conditions in the polar coronal regions are investigated analyzing the brightness and polarization of the 1994 eclipse. We have found that the degree of polarization in polar plumes is about 10% higher than that in the inter-plumes space. Consideration of the brightness in plumes and in the adjacent background space allowed us to conclude that the temperatures there are close to 1 MK. The density in the individual plumes is near $n_0 = 2.7 \times 10^8 \text{ cm}^{-3}$, while it decreases to about $n_0 = 2.0 \times 10^8 \text{ cm}^{-3}$ in the inter-plumes space. It is pointed out that the simultaneous interpretation of the measured brightness and polarization struggles with some difficulties.

Key words: solar eclipse corona – photometry – structuralism – polar plumes – polarization – temperature – density

1. Introduction

Regardless of a number of new and ingenious ground-based and space-borne techniques, experiments and procedures in observing the solar corona, total solar eclipses provide a rare but very valuable opportunity to investigate this uppermost layer of the solar atmosphere with a good resolution and with one of best signal to noise ratio. Such observations are valuable namely when investigating the inner and middle coronal layers up to distances $2 R_{\odot}$, practically inaccessible to current cosmic experiments. Thus, almost all achievements on the

physics of these layers come from the white-light corona eclipse observations, as before.

This paper deals with the results obtained by analysis of observations performed during two solar eclipses which occurred on 3 November 1994 and 11 August 1999. The first one was observed from Criciúma, Brazil ($\lambda = 49^{\circ}22'$ W; $\phi = 28^{\circ}43'$ S) and represents a clearly pre-minimum eclipse, characterized by a very low sunspot activity (the monthly averaged sunspot number was $R = 18$ only for November 1994). The corresponding phase in the cycle (according to Mitchell, 1929) and the flattening of the corona (according to Ludendorff, 1928) were found to be $\Phi = -0.22$ (to calculate it, the necessary data on the moments of the sunspot cycle minima and maxima were taken from ftp://ftp.ngdc.noaa.gov/STP/SOLAR_DATA/SUNSPOT_NUMBERS/maxmin.new) and $\varepsilon = +0.142$, respectively. On the contrary, the second eclipse ($\lambda = 17^{\circ}47'$ E; $\phi = 46^{\circ}55'$ N, Tihany, Hungary) was a typically pre-maximum one, with the August 1999 monthly sunspot number $R = 94$ and displaying an almost circular corona ($\Phi = +0.86$, $\varepsilon = +0.037$). An idea is to look for and to describe the differences in the structuralism and physical conditions arising from the clear qualitative dissimilarities of these eclipses. A short description of observations and quite introductory studies of our white-light images taken during the above two eclipses may be found in Sýkora, Pintér and Ambrož (1995), Sýkora, et al. (1998) and Sýkora (2000).

The white-light images of the eclipse corona provide, first of all, an excellent possibility to estimate a global shape of the solar corona (characterized primarily by the flattening index) and to identify different coronal structures from near the limb to the distance of several Sun's radii. At the same time, the white-light images tell us much about the actual (i.e., related to the eclipse day) global magnetic field topology of the corona. Except of that, the measuring of coronal brightness in the optical continuum is still useful for improving the physical models of the corona, including a more precise estimation of the average coronal temperature and density. The measurement of coronal polarization seems to be particularly valuable for allowing to estimate the density distribution in the corona along the line of sight (i.e., perpendicularly to the plane of sky).

We have studied polarization in the white-light corona earlier (e.g., Badalyan, Livshits and Sýkora, 1997) and a remarkable diversity of this parameter within the different coronal structures was demonstrated. The present paper completes our earlier results with a discussion of the degree of polarization within the polar plumes of the 1994 solar eclipse corona. A close relationship between the characters of the large-scale coronal structures and the Sun's magnetic field has long been recognized (e.g., Howard and Koomen, 1974; Hoeksema et al., 1982; Suess, 1993). We check, demonstrate and discuss such the relationship by comparing the observed coronal shapes and structures with the calculated magnetic field lines of force topology. Our estimation of the magnetic field strength all around the Sun is worth of particular mentioning (a presentation of this kind was firstly introduced by Gibson and Bagenal, 1995). The magnetic field strength and the

form of the corresponding "isogausses" are especially analyzed relatively to the presence of coronal holes close to the solar limb (Sýkora, Badalyan and Obridko, 2003).

Simultaneous interpretation of the coronal brightness and density distributions in the individual coronal structures is of special interest. Such an approach was described by Badalyan and Livshits (1994). In the present paper this method is applied to investigate, namely, the polar plumes of the November 3, 1994 corona.

2. Coronal structures

We usually combine two methods of extracting the structural details from the K+F white-light images of the eclipse corona. One is a well-known procedure of combining the negative and positive of the same original image and mutual turning them for a very small angle. The second way represents the computer contrasting of a given coronal image by a proper software. The contours of a coronal structure as obtained by applying the first method on our eclipse images are shown in Figs. 1 and 2 (left panels). It is evident that the global shape of the 1994 eclipse corona is a typically "minimum-like" one, with coronal streamers being situated close to the solar equator. Owing to a considerably low activity in November 1994 (the monthly averaged sunspot number was $R = 18$), the description of the actual coronal features is relatively simple. Both, the northern and southern poles are occupied by the systems of rays (polar plumes), indicating presence of the open magnetic structures there - coronal holes. The plumes are approximately radial at the poles and increasingly inclined towards solar equator when advancing to the lower latitudes. The polar coronal holes are recognizable on the Yohkoh soft X-ray images recorded at the eclipse day and also on the XUV 17.1 nm image (Fe IX/X), taken by the HAO/NCAR Sounding Rocket.

On the E-limb one major streamer dominates. It takes an unusually large range of latitudes - from position angle 30° to about 130° (position angles are measured counterclockwise from the heliographic north). The streamer is slightly inclined to the N-pole and shows a typical narrowing with height in a cuspidate manner. On the other hand, the streamer seems somewhat heterogeneous. Its brightness and boundaries are not uniform and clearly sharp. It cannot be excluded that this streamer represents a projection of two or even more smaller streamers. This view is supported by the fact that at least five tiny prominence were covered by the streamer during the eclipse.

The W-limb corona is much more structured. First of all, an almost classical well-isolated streamer is visible in the SW-quadrant (at position angles $210^\circ - 250^\circ$), displaying a typical dome structure in its lower part. Two very small prominences are situated eccentrically to the south edge of the streamer's dome. By the way, the prominences inside the streamer's dome are typically seen when

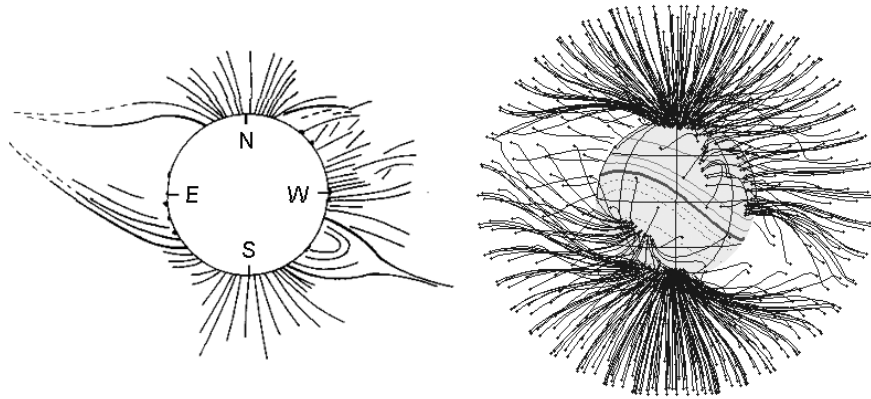


Figure 1. Contours of the November 3, 1994 eclipse corona structure (left) and calculated magnetic field lines for the same eclipse day (right).

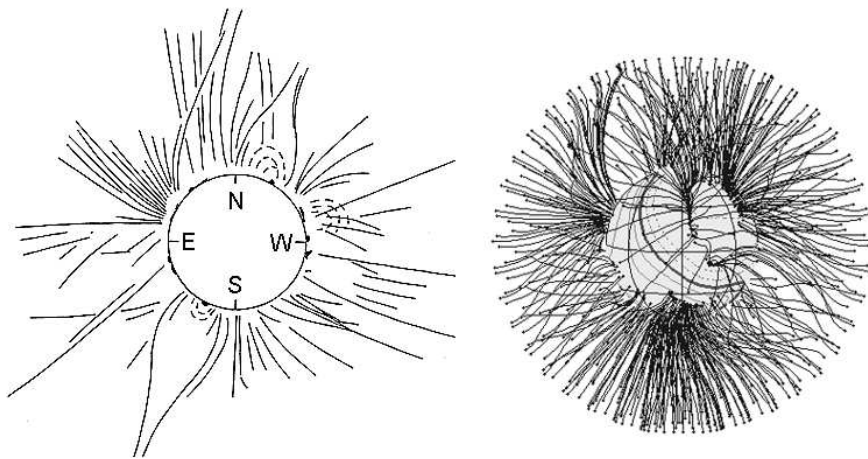


Figure 2. The same as in Fig. 1, but now for the August 11, 1999 solar eclipse.

the streamer is situated close to the solar limb. Continuing to the solar north, a faint decrease of coronal brightness takes place around the equator, followed by a higher activity in the middle part of the NW-quadrant. Also here the solar corona exhibits, at least, some indication of the streamer. Its apparently undeveloped structure is because the streamer's anchorage is still well on the Sun's visible hemisphere and, therefore, projection of the streamer onto the 2D plane of the sky cannot be well-pronounced.

The global shape of the 1999 corona substantially differs from that of the 1994 one (Fig. 2). In this case the streamers are seen nearby the Sun's poles. The

loop-like domes at the SE- and NW-streamer's base, with a small prominence inside are typical for the streamer architecture. Some traces of polar plumes are present at lower latitudes of the E- and W-limb. Generally, the streamers are situated over the solar magnetic equator (e.g., Koomen, Howard and Michels, 1998; Wang, Sheeley and Rich, 2000; Sýkora, Badalyan and Obridko, 2003) which, close to the solar cycle maximum, is highly inclined with respect to the heliographic equator and indicates forthcoming reversal of the global magnetic field of the Sun. Therefore, it should be expected that the pronounced facts would be confirmed by the corresponding calculations of the magnetic field structure and its topology. Considering an open ray-like structure at the middle latitudes of the 1999 eclipse E-limb, a coronal hole is anticipated to be present in that region. A mutual relation of the calculated magnetic field strength and the presence of this coronal hole is discussed below particularly. A broader meaning of such a relation is outlined, as well.

In the right panels of Figs. 1 and 2 the systems of the magnetic field lines of force are presented, as derived for the days of both considered eclipses. The calculations were performed under a potential approximation using the photospheric field measurements of the Wilcox Solar Observatory. The method of computation (and the field presentations for 10 solar eclipses) are described in Sýkora, Badalyan and Obridko (2003). There and here, we have applied the well-known method, earlier described by Hoeksema and Scherrer (1986), and Hoeksema (1991). Some details about our calculations can be also found in Sýkora et al. (1999). This approach assumes that the magnetic field energy in the layers between the photospheric surface and a certain level in the solar corona is higher than the energy of the possible electric currents. In other words, the deviations of the magnetic field structure from a potential character of the field are assumed to be small and, we neglect them. However, starting from a certain height, the flows of the solar wind plasma are no longer negligible, the field cannot be any longer considered current-free and the field lines of force are gradually stretched to a practically radial direction. The surface, where the lines of force are supposed to be strictly radial is used to be called the source surface. In Hoeksema and Scherrer (1986) this radius was taken to be $2.5 R_{\odot}$, and the same value was utilized throughout all our calculations. The calculations involved summing over 10 harmonics and introducing a polar correction to take into account the lack of reliability of the field measurements in the vicinity of the solar poles (Obridko and Shelting, 1999).

The mentioned calculations provide the magnetic field lines of force usually well-describing presence and distribution of the large-scale structures in the solar corona, mainly, helmet streamers and coronal holes (e.g., Sýkora, Badalyan and Obridko, 2003). For example, in the right panel of Fig. 1 the east and west equatorial streamers well visible in the structure drawing of the 1994 eclipse are clearly expressed also in the magnetic field structure. In the same panel also distinct open structures close to the poles are remarkable. On the contrary, the 1999 eclipse represents an example of not very convincing description of the

coronal structures by the magnetic field lines of force (right panel in Fig. 2). A certain correspondence of these two presentations is seen only in the north-pole region.

One should have in mind that all the visible and above-described coronal structures are not necessarily situated directly at the solar limb. The eclipse images and the derived from them sketches of the coronal structures represent at each moment a 2D-projection only of the real 3D-shape of the corona to the plane of the sky. Namely, the streamers may be well seen in the 2D-projection though anchored to the photosphere relatively far from the limb. This "observational inadequacy" of the eclipses led, in fact, to a historically false estimations of the global coronal shape evolution throughout the solar cycle (Sýkora, Badalyan and Obridko, 2003). We now believe that the 3D-corona is always considerably flattened, but with regard to the equator of the global Sun's magnetic field. In fact, any calculations of the coronal flattening with regard to the heliographic equator seem to be pretty much incorrect, namely well outside the solar cycles minima when the two above equators are considerably inclined to each other (Gulyaev, 1992, 1994; Sýkora and Badalyan, 1992).

3. Brightness and polarization of the white-light corona

Following photometric processing of the coronal images taken during the 1994 and 1999 eclipses the isolines of brightness (isophotes) were constructed. In the left panel of Fig. 3 the isophotes of the 3 November 1994 corona are drawn in some relative units. Difference between the isolines is $\Delta \log I = 0.25$. As this figure demonstrates, the coronal isophotes delineate well the large-scale structures of the corona only. The large helmet streamers are expressed - one at the east and two at the west limbs. In the polar regions the structures are practically unresolved by the isophotes. In the distance of about $2 R_{\odot}$ the isolines of brightness become almost circular. In these distances the basic input to the observed brightness comes from the F-corona, always displaying a small flattening.

The form of the solar corona has long been determined by the Ludendorff flattening coefficient. It is defined as:

$$\varepsilon = \frac{d_e}{d_p} - 1, \quad (1)$$

where d_e and d_p are the equatorial and polar distances of the same isophote, and obtained as the means of the values at three positions: 0° , $\pm 22.5^\circ$ and 90° , $90^\circ \pm 22.5^\circ$, respectively. The isophote at 0° is recommended to be chosen at the distance of about $2.0 R_{\odot}$. Calculation according to this formula gives $\varepsilon = +0.142$ for the 1994 eclipse corona flattening. The minimum-type corona was not quite well-developed at the moment of this eclipse (the Sun's magnetic equator was still noticeably wavy in relation to the heliographic equator) and, therefore, the found flattening value is lesser in relation to the classically expected one.

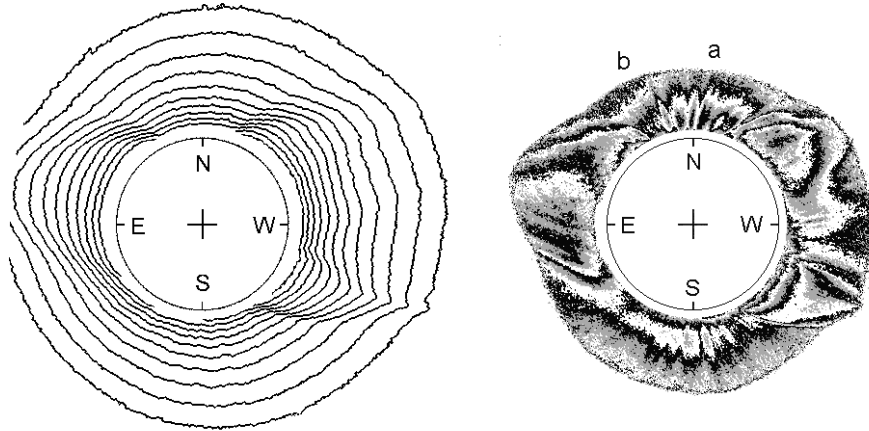


Figure 3. The isolines of brightness (left) and the degree of polarization (right) of the 1994 corona. The step between two adjacent isolines of brightness is $\Delta \log I = 0.25$, and the difference between the neighbor shadowing of the degree of polarization represents $\Delta p = 5\%$.

On the right in Fig. 3 the lines of equal polarization (isopleths) of the white-light corona are presented. Each of the bands (white, gray, and dark) covers an interval of the degree of polarization in extension of $\Delta p = 5\%$. For example, the outer gray strip over the north and south poles corresponds to the polarization of 20 – 25%, the following black belt covers the polarization of 25 – 30%, etc. The highest polarization is found inside the large helmet streamers and is more than 55% (black regions inside the streamers). In difference from the system of isophotes (the left part of this figure) the isolines of equal polarization display much more distinctly the individual characteristic structures of the 1994 corona. So, analyzing the right panel of Fig. 3 one can assume that the southwest streamer is slightly out of the image plane, its equator-ward part is situated closer to the plane of the sky (that is why it exhibits a higher degree of polarization) in comparison with its southern part. In the polar regions the polar plumes are well visible. The degree of polarization in these plumes is for about 10% higher than in the inter-plumes space. The highest degree of polarization in the polar plumes is typically rather low at the distances $1.25 - 1.30 R_{\odot}$. We assume that the northern and southern polar plumes are unlikely inclined to the plane of the sky because the highest degree of polarization inside them is situated at different distances. Such view of the polarization allows to identify even fine structural details, for example, small-size rays around the west equator (see also Sýkora, Badalyan and Obridko (2003), where the polarization of the 11 July 1991 corona is described).

Fig. 4 makes possible to compare the polarization of the 1994 white-light

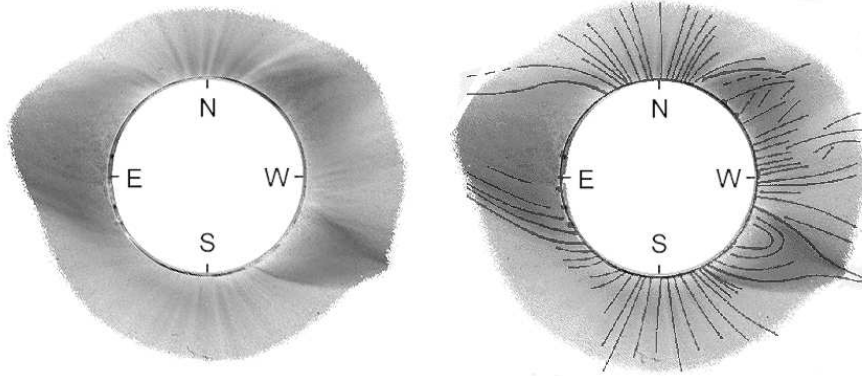


Figure 4. An image of the 1994 corona polarization distribution (left) - the darker shadowing corresponds to the higher degree of polarization. On the right panel, the structures of Fig. 1 overlay the image of the polarization distribution.

corona with the structural sketch of this corona. Polarization in this figure is not given in the form of isopleths as it was in Fig. 3, but in the means of polarization itself, in absolute units. The darker the corresponding regions, the higher the polarization. White color in such a pattern corresponds to absence of polarization ($p = 0\%$), while black color would represent the total polarization ($p = 100\%$). This kind of a polarization chart distinctly displays characteristic coronal structures, as well. Particularly, the fine polar plumes are visible here in the form of small darker structures with a brighter background around them. Right in this figure is a sketch of the coronal structures (presented in the left panel of Fig. 1) superimposed on the chart of the degree of polarization. One may agree that the coronal structures quite well correspond to the polarization. Thus, the polarization chart of the 1994 eclipse confirms our earlier finding (Badalyan, Livshits, Sýkora, 1997; Badalyan, Obridko, Sýkora, 2003) that the polarization considerably better reflects details of the coronal structures than the isophotes do. This is connected with the fact that within the visible eclipse corona structures (among them, helmet streamers and polar plumes) the matter is understandably somewhat concentrated to the plane of the sky what results in increase of the measured degree of polarization in these structures.

The same conclusions follow from Fig. 5 displaying the isophotes and isopleths for the 11 August 1999 eclipse. The isophotes are here, similarly to the left panel of Fig. 3, given in the relative units, the difference between the adjacent isophotes being $\Delta \log I = 0.25$. This figure indicates that the isophotes become almost circular already at small distances from the solar limb during a majority of the eclipses appearing in the periods of the solar cycle maxima. The reasons for exceptions from this rule were discussed earlier (e.g., Sýkora and Ambrož, 1995;

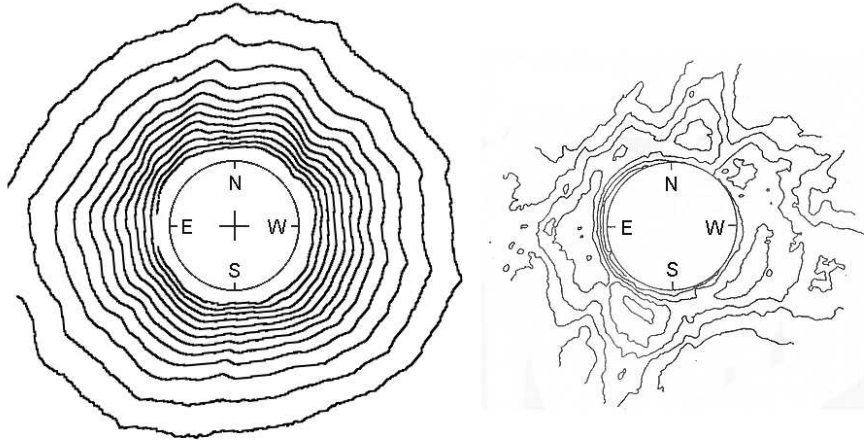


Figure 5. Isophotes of the 1999 corona, the step between two adjacent isolines of brightness being $\Delta \log I = 0.25$. On the right panel of this figure are the isolines of polarization (isopleths), as obtained in the frame of European TECONet Project (also with our participation) and taken from Clette and Gabryl (1999). Maximum polarization in streamers of the 1999 corona reaches up to 45%, the difference between the adjacent downwards isopleths being $\Delta p = 5\%$.

Sýkora, Badalyan and Obridko, 2002). The solar corona of the 1999 eclipse does not exhibit any expressive large-scale structures. Only the moderate dimension streamers are noticeable in the figure of isolines. The flattening of the 1999 corona is $\varepsilon = +0.037$ only, corresponding well to the classically expected one during the near-maximum phase of the activity cycle (in the case of this 1999 eclipse a quadruple of the global magnetic field was present on the Sun and the heliomagnetic and heliographic equators were mutually highly inclined).

Right in Fig. 5 the isolines of the degree of polarization are demonstrated in a classical way. These isopleths were derived by Clette and Gabryl (1999) in the frame of the European TECONet Project (one of the authors - J.S. - has participated in this Project, as well), the difference between the adjacent isolines being $\Delta p = 5\%$. The highest polarization arises within the streamers at distances $1.4-1.5 R_{\odot}$ and goes up to 45%. This is a typical degree of polarization for the large dimensional streamers.

4. Temperature and density in the corona

4.1. About our method of determination the temperature and density in the corona

A method to determine the temperature and density in the solar corona was proposed by Badalyan (1988, 1995). In the frame of the accepted model of the density distribution a set of theoretical curves of the $\ln(K_t + K_r)$ in dependence on $1/\rho$ (where K_t and K_r are polarized components of radiation, and ρ is the distance from the solar disk center) is constructed. In the quoted papers, all the calculations were performed assuming the hydrostatic density distribution found earlier from observations of a number of investigators for the middle corona (see, for example, Newkirk, 1967). We should underline that such a statement does not insist upon absence of any motions in the corona. It simply means only that these motions are of low velocities or that their fraction is small and due to this they do not manifest themselves in the observed density distribution of these coronal layers. The basic calculations were performed for the densities at the base of the corona (more exactly, of the hydrostatic law parameter) $n_0 = 10^8 \text{ cm}^{-3}$.

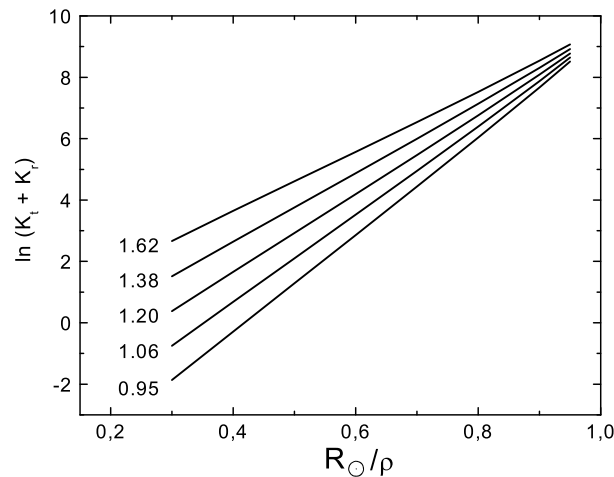


Figure 6. A family of theoretical lines representing dependence of the K-corona brightness on distance from the Sun's disk center. Calculations were performed for different temperatures (they are indicated in this figure in MK) and for density at the base of corona $n_0 = 10^8 \text{ cm}^{-3}$, representing a parameter of the hydrostatic law.

Fig. 6 shows a family of the theoretical curves $\ln(K_t + K_r)$ for a set of temperature values (they are identified in the figure) and for the density of the corona at its base $n_0 = 10^8 \text{ cm}^{-3}$. This figure shows that inclination of the theo-

retical curve increases with the decreasing coronal temperature. The method of the temperature and density determinations consists in the following. The observed dependence of the K-corona brightness on $1/\rho$ (i.e., after subtraction of the F-corona from the white-light corona) is superimposed on the family of the theoretical curves. The density enters exponentially into equations describing the theoretical values of the tangential and radial components of the polarized radiation K_t and K_r . Therefore, the found shift of the K-corona brightness values along the ordinate direction allows us to deduce on the density at the base of the solar corona. The quantities T and n_0 make it possible to derive the density at any distance under the accepted assumptions.

This method was utilized by Badalyan (1988, 1995) for a number of eclipse observations performed by different authors. It has been shown that the observed course of brightness at the heights of the middle (and partially also of the inner) corona agrees, with astonishing stability and independently on the phase of activity cycle, with the theoretical brightness calculated for the hydrostatic distribution of density. It has been also obtained that the temperature within the equatorial regions of the middle corona steadily remains around 1.4 MK. We note that the same temperature for these coronal regions was announced long ago by Alfvén (1941). Apparently, this is connected with a general balance of energy throughout the solar corona. The density changes in dependence on the phase of activity cycle from $n_0 = 2 \times 10^8 \text{ cm}^{-3}$ in the minimum of solar activity to $n_0 = 4 \times 10^8 \text{ cm}^{-3}$ in the cycle maximum. Within the polar coronal holes the temperature depends on the cycle phase. During the solar maximum it corresponds to the temperature in the equatorial regions and is close to 1.4 MK, while at the solar minimum it decreases to 0.9–1.0 MK. The density does not exhibit any clear cycle phase dependence and, possibly, is connected with the properties (e.g., dimensions) of the polar hole itself (these our results are quoted by Golub and Pasachoff (1997), p. 139).

Badalyan (1988, 1995) concluded that the course of brightness over the layers of the quiet middle corona represents such a stationary parameter that it can serve as a test of "quality" of the performed eclipse observations. For example, the observational data (usually, the images) obtained during one and the same solar eclipse may contain some observational peculiarity (let's say, an inadequacy) at all position angles, differing from the data peculiarity of some another author. The above mentioned uniformity in the course of the K-corona brightness makes then possible: (a) to make a more precise absolute calibration of the eclipse observations using the model of the F-corona as a photometric standard. Comparison of the data obtained by different authors during one and the same solar eclipse (Badalyan 1988, 1995) has revealed that these data really contain a certain (different for individual authors) error in the absolute calibration of them. After including some correction (using the F-corona in term of the photometric standard and consecutive subtraction of it from the total brightness) all the data considerably better fit one and the same theoretical curve; (b) to derive with a satisfying accuracy the absolute calibration of those

observations for which the calibration during an eclipse wasn't done, or is incorrect. This can be done by using the F-corona model and taking into account the known from the model (for example, of the Van de Hulst model, or of any similar model) contribution of the K-corona into the total coronal brightness at the distances around $2 R_{\odot}$. Below, when interpreting the observations of the 1994 and 1999 coronae, we exploited the above possibility.

The described method of the temperature and density determinations has been employed by Gabryl, Cugnon, and Clette (1997), and Kulijanishvili, and Kakhiani (1996) who confirmed the conclusions of Badalyan (1988, 1995). We should add that for the distances above $2 - 2.5 R_{\odot}$ the model of the hydrostatic density distribution is not further usable. At these distances the power of gravity decreases and the gas pressure in the hot corona remains to be high. The gravity (and some other powers, e.g., magnetic one) is not further able to keep the hot gas and a hydrostatic flow of the coronal plasma comes into being, creating a quiet solar wind.

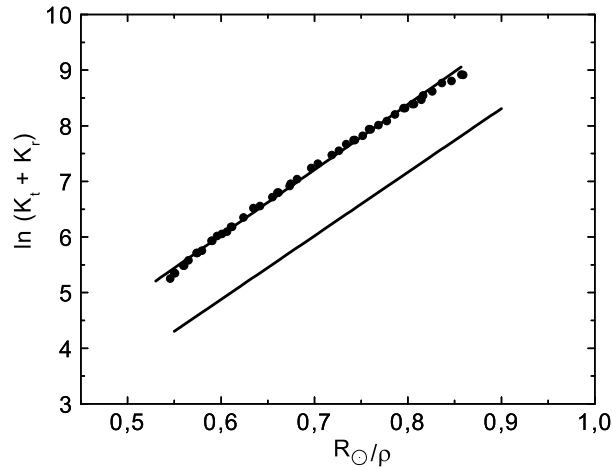


Figure 7. The measured course of the brightness within the equatorial region of the 1999 corona (at the position angle 105°). The measurements are indicated by points, together with a linear approximation of the corresponding course. The lower line represents a theoretical dependence obtained for 1.4 MK temperature and $n_0 = 10^8 \text{ cm}^{-3}$ density. The shift of the observed dependence along the ordinate with respect to the theoretical line corresponds to the coronal density $n_0 = 3.3 \times 10^8 \text{ cm}^{-3}$.

4.2. Temperature and density of the corona during solar activity maximum

Fig. 7 demonstrates a comparison of the observed distribution of brightness within the equatorial 1999 corona (the points and approximation straight line of them) with the theoretical dependence derived for the temperature $T = 1.4$ MK and the density $n_0 = 10^8 \text{ cm}^{-3}$ (the lower line). The observed distribution is drawn for the region of a quiet corona at position angle $P = 105^\circ$. To bring our measurements of brightness to the photometric standard the model of F-corona by Koutchmy and Lamy (1985) was used. In agreement with the Van de Hulst model (1950) we have adopted that at the distances around $2 R_\odot$ the K-corona represents about 0.6 portion of the total coronal brightness. Estimation of this portion makes it possible to calculate the standardization multiplier by which the relative brightness should be multiplied for each point of the corona to transform the data into the absolute units. Then, the logarithm of the absolute coronal brightness at the distance $2 R_\odot$ of the given position angle is $\log I = 2.4$ (in the units 10^{-10} of the Sun's disk center brightness). The uncertainty in determination of this value does not exceed 0.1-0.15. Adoption of a multiplier for transformation to the absolute values was tried for a number of position angles to choose this multiplier with sufficient accuracy.

Fig. 7 indicates that at the position angle in question, the brightness distribution is close to that obtained under the assumption of the hydrostatic density distribution. The straight line inclination for the observed K-corona corresponds to the temperature 1.4 MK. The necessary shifting of the observed dependence along the ordinate axis is upwards with regard to the theoretical one and represents $\Delta \ln(K_t + K_r) = 1.2$, giving the density of $3.3 \times 10^8 \text{ cm}^{-3}$ at the base of corona. At the distance $1.5 R_\odot$ of the position angle in question the density of the quiet corona is $1.35 \times 10^7 \text{ cm}^{-3}$, considering the hydrostatic density distribution. The obtained temperature and density values are in agreement with all other values obtained by Badalyan (1988, 1995) for the regions of the quiet equatorial corona in the period of solar cycle maximum.

5. Physical conditions within the polar plumes of the November 3, 1994 corona

In this section we discuss the physical conditions inside an individual polar plume and in the plumes background of the November 3, 1994 corona. The polar plume is situated close to the position angle $P = 355^\circ$. In Fig. 3 this plume is denoted by "a" (the dark small grains at the distance $1.2-1.3 R_\odot$). The brightness of the K-corona along this plume is given in the left panel of Fig. 8. The polarization in the plume reaches a maximum at the distance $1.25 R_\odot$, slightly exceeding 40% (see the left panel in Fig. 9). The polar corona outside the polar plumes (the background corona) is analyzed at $P = 21^\circ$. In Fig. 3 this angle is indicated by "b". The brightness and polarization for this position are

given in Figs. 8 and 9 (in the right panels of them). In this inter-plume space the maximum of polarization decreases to about 30%.

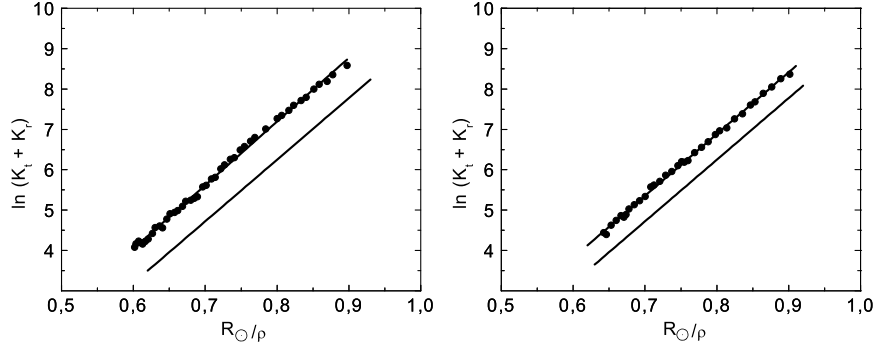


Figure 8. The measured course of brightness within the polar plume (left panel; in Fig. 3 this plume is indicated by "a"), and in the inter-plume space (right panel; in Fig. 3 the chosen space is designated by "b") of the 1994 corona. The theoretical dependence (the lower lines in both panels) are calculated assuming temperature of 1 MK. The magnitude of shifts along the ordinate of the observed dependence with respect to the theoretical dependence corresponds to the coronal densities $n_0 = 2.7 \times 10^8 \text{ cm}^{-3}$ in the plume and $n_0 = 2.0 \times 10^8 \text{ cm}^{-3}$ in the inter-plume space.

The theoretical dependence (lower lines in Fig. 8) is derived for the temperature of 1 MK. As above, using of the Koutchmy and Lamy F-corona model (1985) for the polar region allowed us to calibrate the observed data in the absolute units. In the polar regions, according to the model of Van de Hulst (1950), the contribution of the K-corona to the total coronal brightness represents only 0.1 at the distance $2R_\odot$. It is obvious from Fig. 8 that the course of brightness throughout the polar corona, both in the plume and in the background of plumes, corresponds to a hydrostatic density distribution. This means that no influence of the motions is detected at these distances. The inclinations of the dependence correspond to the theoretical straight line related to 1 MK. The shifting (along the ordinate direction) of the experimental dependence in relation to theoretical ones (the lower lines in Fig. 8) provide the plume density $n_0 = 2.7 \times 10^8 \text{ cm}^{-3}$ and the inter-plume space density $n_0 = 2.0 \times 10^8 \text{ cm}^{-3}$. At the distance $1.5R_\odot$ the densities in the plume and in the plume's background are $2.7 \times 10^6 \text{ cm}^{-3}$ and $2.0 \times 10^6 \text{ cm}^{-3}$, respectively. This means that at these distances the density in the plume and in the plume's background decreases by one hundred times in comparison with their n_0 values at the corona base.

The obtained distributions of the coronal brightness and polarization permit us to give their simultaneous interpretation. Possibility of such interpretation was discussed earlier by Badalyan and Livshits (1994) and Badalyan, Livshits

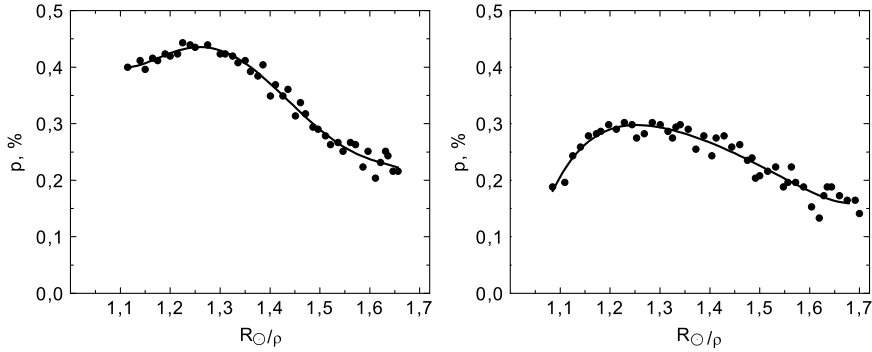


Figure 9. The measured course of the degree of polarization over the polar plume (left) and in the inter-plume space (right) of the 1994 corona.

and Sýkora (1997). This assumes to look for a model in the frame of which a simultaneous explanation of the course of brightness and polarization is possible. The temperatures and densities found within the plume and in the inter-plume space make it possible to calculate the theoretical values of the degrees of polarization in these structures and then to compare them with the observational measurements.

Polarization of the (K+F)-corona is expressed as:

$$p = \frac{K_t - K_r}{K_t + K_r + F}, \quad (2)$$

where F represents the brightness of the F-corona. The equations for calculation of the polarized components of radiation K_t and K_r in the case of the hydrostatic density distribution were derived by Badalyan (1986).

The calculations indicate that for the inter-plume background the model of a spherically symmetric corona is adequate. Then for the density in this background $n_0 = 2.0 \times 10^8 \text{ cm}^{-3}$, the temperature 1.0 MK and the brightness of the F-corona taken from the Koutchmy and Lamy (1985) model, we obtain the polarization $p = 29.9\%$, well in agreement with our observational findings.

For the plume itself the model is adopted in which a narrow dense plume is embedded by a spherically symmetric background. This means that the polar plume is situated close to the plane of sky, in front of the plume and behind it a spherically symmetric background exists characterized by the hydrostatic parameter of density $n_0 = 2.0 \times 10^8 \text{ cm}^{-3}$. In such a model the polarization is expressed as follows:

$$p = \frac{(K_t - K_r)_b + (K_t - K_r)_p}{(K_t + K_r)_b + (K_t + K_r)_p + F}, \quad (3)$$

where $(K_t + K_r)_b$ and $(K_t - K_r)_p$ are, respectively, the sum and difference of the polarized components of radiation in the background, and $(K_t + K_r)_b$ and $(K_t - K_r)_p$ are the same inside the polar plume. Integration within the plume is done according to the same equations taken from Badalyan (1986), but along a short interval of distances close to the plane of sky only. Understandably, for the plume background the integral is calculated from "a rest" interval of distances, i.e., from the minus to plus infinity along the line of sight, with exclusion of that part of distances where the plume occurs. "The infinity" here is, of course, conditional. The density rapidly decreases, at a certain distance from the plane of sky it is negligible and contributes very little to the calculated integral. The density inside the plume, representing a denser structure, is higher in comparison with the plume's background. This means that the coronal matter in this case is really concentrated towards the plane of sky. As it was shown by Badalyan and Livshits (1994) and Badalyan, Livshits and Sýkora (1997), the polarization in such a model is higher in comparison with that following from the spherically symmetric model of the solar corona.

We adopted that extension of the plume along the line of sight approximately corresponds to its crosswise dimension in the plane of image. We have also assumed that the density inside the plume is five times larger of that in the background. Such a ratio of densities follows from the past observations and was quoted by Shklovskii (1962, p. 444). As emerged, in our case namely such a relation of the densities inside the plume and in the plume surroundings corresponds to the observed brightness of the polar coronal plume and, thus, to the density $n_0 = 2.7 \times 10^8 \text{ cm}^{-3}$. The calculations according to equation (3), assuming $n_0 = 2.7 \times 10^8 \text{ cm}^{-3}$ density, gave us polarization 32.6%. This is less enough in comparison with observed value of about 40%.

A dense plume, characteristic by the observable brightness and complete absence of the background radiation, could represent the limiting case. This would be true if all the matter assumed along the line of sight is concentrated into the narrow plume only, situated close to the plane of the sky. Then, only the terms with the "p" index will remain in equation (3). The density $n_0 = 3.5 \times 10^9 \text{ cm}^{-3}$ is necessary to be assumed to obtain in this case the observed polar plume brightness. In this case the calculations offer the degree of polarization as much as 35.1% which is still smaller than that measured from the eclipse images. As it follows from equation (3) to obtain a higher degree of polarization of the (K+F)-corona it is still necessary to enlarge somewhat the plume density. Our calculations show that the observed polarization could be obtained only in the case of about three times higher brightness than really observed. Therefore, in the case of the polar coronal plume we are not able satisfactorily concord the measured degree of polarization with the observed course of the coronal brightness. The brightness of the plume appears to be insufficient for explanation of the observed polarization inside it.

6. Conclusion

In this paper we discuss the photometric processing and provide interpretation of the results coming from ground-based observations of the November 3, 1994 and August 11, 1999 total solar eclipses.

Distribution of the white-light solar corona brightness during the 1999 eclipse, occurring close to the period of solar cycle maximum, confirmed the earlier obtained conclusions indicating temperature of about 1.4 MK within the equatorial regions of the lower and middle corona over the distances from about $1.2 R_{\odot}$ up to $2.0 R_{\odot}$. Distribution of the coronal density is nearly hydrostatic, acquiring the value $3.3 \times 10^8 \text{ cm}^{-3}$ at base of the corona (this being a parameter of the hydrostatic law). The 1994 eclipse happened rather close to the minimum of solar activity. The coronal structure of this eclipse displays a typical minimum form with the well-developed polar plumes. A careful processing of the eclipse images provided quite a good impression on the course of polarization along the narrow polar plumes (to our knowledge, namely this represents an original finding). Maximal degree of polarization in the polar plumes goes to 40% at the distances $1.25 - 1.3 R_{\odot}$ from the disk center, which for about 10% exceeds the polarization within the inter-plumes space. The brightness distribution in the polar plumes and in the space between them corresponds to the 1 MK temperature throughout the polar solar corona. The density at the base of the inner background corona is $2.0 \times 10^8 \text{ cm}^{-3}$, while within the polar plume it reaches $2.7 \times 10^8 \text{ cm}^{-3}$.

The simultaneous interpretation of the brightness and polarization within the polar plume and outside makes it possible to construct a certain model of these features. The courses of the brightness and polarization over the polar region of the November 3, 1994 corona correspond to the model of the spherically symmetric corona. The mean density in the region where the plume is situated is for 1.35 times higher than that outside the plumes. We have tried the model in which the narrow plume is in a projection with the coronal background, the density of the plume being 5 times higher than that in the background. Such a structure in which the matter is concentrated towards the plane of the sky results in an enlargement of polarization for several percents. However, we are not successful in simultaneous explaining of the 10% difference in polarization and of the observed brightness distribution. On the other side, Badalyan and Livshits (1994) showed that in the case of a typical coronal streamer the simultaneous interpretation of the brightness and polarization is possible, even up to the relatively large distances. Some difficulties occur when constructing the model of huge streamers similar to that observed during the 1952 solar eclipse. It becomes evident that the brightness within large plumes is insufficiently high to give the observed degree of polarization. The same problem appeared in our present study of the polar plume.

However, in our opinion, the found contradiction does not represent now a sufficiently significant reason for any revision of the mechanism of the white-

light corona radiation, or looking for some alternative explanations of the origin of an additional polarization in the polar plumes. It should be noted that the measurements of polarization are rather difficult and for any new theoretical constructions the very relevant results should be introduced. Therefore, it is still valuable to continue in the careful observations of coronal polarization to obtain more important reasons, if the present theory of polarization should be questioned.

Acknowledgements. This investigation was supported by the Project 05-02-16090 of the Russian Foundation for Basic Research, the Scientific School 8499.2.006.2, and by VEGA Grant No. 2/7012/27 of the Slovak Academy of Sciences.

References

- Alfvén H.: 1941, *Arkiv Mat. Astron. Phys.* **27A**, N 25
- Badalyan, O.G.: 1986, *Astron. Astrophys.* **169**, 305
- Badalyan, O.G.: 1988, *Fizika Solnechnoj aktivnosti*, Nauka, Moscow, p. 88 (in Russian)
- Badalyan, O.G.: 1995, *Astron. Astrophys. Transact.* **9**, 205
- Badalyan, O.G., Livshits, M.A.: 1994, in *Solar Coronal Structures*, eds.: V. Rušin, P. Heizel and J.C. Vial, Veda, Bratislava, 77
- Badalyan, O.G., Livshits, M.A., Sýkora, J.: 1997, *Solar Phys.* **173**, 67
- Clette, F., Gabryl, J.-R.: 1999, *ESA SP 448*, 1273
- Gabryl, J.-R., Cugnon, P., Clette, F.: 1997, in *Theoretical and Observational Problems Related to Solar Eclipses*, eds.: Z. Mouradian and M. Stavinschi, Kluwer, Dordrecht, 73
- Gibson, S.E., Bagenal, F.: 1995, *J. Geophys. Res.* **100**, No. **A10**, 19865
- Golub, L., Pasachoff, J.M.: 1997, *The Solar Corona*, Cambridge Univ. Press, Cambridge
- Gulyaev, R.A.: 1992, *Solar Phys.* **142**, 213
- Gulyaev, R.A.: 1994, *Astrophysical J.* **437**, 867
- Hoeksema, J.T.: 1991, *Solar Magnetic Fields - 1985 through 1990*, Report CSSA-ASTRO-91-01, Center for Space Science and Astronomy, Stanford University
- Hoeksema, J.T., Scherrer, P.H.: 1986, *The Solar Magnetic Field - 1976 through 1985*, WDCA Report UAG-94, NGDC, Boulder
- Hoeksema, J.T., Wilcox, J.M., Scherrer, P.H.: 1982, *J. Geophys. Res.* **87**, 10331
- Howard, R.A., Koomen, M.J.: 1974, *Solar Phys.* **37**, 469
- Koomen, M.J., Howard, R.A., Michels, D.J.: 1998, *Solar Phys.* **180**, 247
- Koutchmy, S., Lamy, P.L.: 1985, in *Properties and Interactions of Interplanetary Dust*, eds.: R.H. Giese and P. Lamy, Reidel, Dordrecht, 63
- Kulijanishvili, V.I., Kakhiani, V.O.: 1996, *Romanian Astron. J.* **6**, 9
- Ludendorff, H.: 1928, *Sitzber. Preuss. Akad. Wiss.* **16**, 185
- Mitchell, S.A.: 1929, *Handb. Aph.* **4**, 231
- Newkirk, G. Jr.: 1967, *Ann. Rev. Astron. Astrophys.* **5**, 812
- Obridko, V.N., Shelting, B.D.: 1999, *Solar Phys.* **184**, 187
- Shklovskii, I.S.: 1962, *Physics of the Solar Corona*, Fizmatgiz, Moscow, (in Russian), transl. 1965, Pergamon Press, Oxford
- Suess, S.T.: 1993, *Adv. Space Res.* **13**, 31

- Sýkora, J.: 2000, in *The 15th Meeting on Solar-Terrestrial Physics*, ed.: B. Lukáč, SUH, Hurbanovo, 160, (in Slovak)
- Sýkora, J., Ambrož, P.: 1995, in *24th International Cosmic Ray Conference*, ed.: N. Iucci, IUPAP, Roma, 509
- Sýkora, J., Ambrož, P., Minarovjech, M., Obridko, V.N., Pintér, T., Rybanský, M.: 1998, in *Solar Jets and Coronal Plumes*, ed.: T.-D. Guyenne, ESA SP-421, Noordwijk, 79
- Sýkora, J., Badalyan, O.G.: 1992, in *Proc. of the First SOHO Workshop "Coronal Streamers, Coronal Loops, and Coronal and Solar Wind Composition"*, ed.: C. Mattok, ESA, ESTEC, Noordwijk, 137
- Sýkora, J., Badalyan, O.G., Obridko, V.N.: 2002, *Adv. Space Res.* **29**, 395
- Sýkora, J., Badalyan, O.G., Obridko, V.N.: 2003, *Solar Phys.* **212**, 301
- Sýkora, J., Badalyan, O.G., Obridko, V.N., Pintér, T.: 1999, *Contrib. Astron. Obs. Skalnaté Pleso* **29**, 89
- Sýkora, J., Pintér, T., Ambrož, P.: 1995, in *Proc. Int. Symp. on the Total Solar Eclipse of November 3, 1994*, eds.: M.S. Raljevic, F. Zaratti and J.M. Pasachoff, Revista de la Academia Nacional de Ciencias de Bolivia No. 69, La Paz, 23
- Van de Hulst, H.C.: *Bull. Astron. Inst. Netherland, 1950* **11**, 135
- Wang, Y.-M., Sheeley, N.R., Jr., Rich, N.B.: 2000, *J. Geophys. Res. Lett.* **27**, 149